In vitro biomechanical modulation-retinal detachment in a box.

Ghosh, Fredrik; Arnér, Karin; Taylor, Linnéa

Published in:
Graefe's Archive for Clinical and Experimental Ophthalmology

DOI:
10.1007/s00417-015-3236-3

2016

Document Version:
Peer reviewed version (aka post-print)

In Vitro Biomechanical Modulation - Retinal Detachment In a Box

Fredrik Ghosh, Karin Arnér, and Linnéa Taylor
Department of Ophthalmology, Lund University Hospital, Lund, Sweden

Corresponding author:
Linnéa Taylor
Department of Ophthalmology
Lund University Hospital
S-22184 Lund, Sweden
phone:+46 46 2220752
fax: +46 46 2220774
e-mail: linnea.taylor@med.lu.se

Supported by: The Faculty of Medicine, University of Lund, The Swedish Research Council, The Carmen and Bertil Regnér Foundation, The King Gustaf V and Queen Victoria Freemason Foundation, The Foundation of Debilitating Eye Diseases in former Malmöhus County.

ABSTRACT

Background: To illustrate the importance of biomechanical impact on tissue health within the central nervous system (CNS), we here describe an in vitro model of rhegmatogenous retinal detachment (RRD) in which disruption and restoration of physical tissue support can be studied in isolation. Methods: Adult retinal porcine explants were kept in culture for 3 or 12 hours without any tissue support, simulating clinical RRD, after which they were either maintained in this state or reattached to the culture membrane for an additional 48 hours. Results: In vitro detachment resulted in gliosis and severe progressive loss of retinal neurons. In contrast, if the explant was reattached, gliosis and overall cell death was attenuated, ganglion cell death was arrested, and the number of transducin expressing cone photoreceptors increased. Conclusions: These results support the hypothesis that removal of the elastic retina from its normal physical environment results in degenerative damage, and, if restored, rescues retinal neurons. Our study reinforces the notion of a strong relationship between the biomechanical environment and homeostasis within the retina which has significant bearing on pathologic events related to RRD, and may also have impact on other regions within the CNS under biomechanical influence.

Keywords: Retinal biomechanics, retinal detachment, gliosis, Müller cell, ganglion cell

INTRODUCTION

The field of biomechanics, i.e the study of biological entities in relation to their mechanical properties, has traditionally focused on macroscopic explorations of the musculoskeletal and cardiovascular systems. However, the discovery of mechanotransduction (the conversion of mechanical stimuli to biochemical signaling) as an important regulator of cell and tissue homeostasis has led to a more generally applicable paradigm in which biomechanics come into play on the nano-, cell- and tissue-scale [1]. The biomechanical system including mechanoreceptors, ECM and cytoskeleton is an integral part of the normal tissue continuum the integrity of which is of importance throughout the body. Perturbation of mechanotransduction - related signaling is therefore by nature very rapid, and if sustained, may be an important initiator of disease.

The retina is a part of the central nervous system (CNS), and, in similarity to the brain, consists of a highly organized neuronal network residing within a biomechanical milieu. The retinal sheet is subjected to adhesive force from the vitreous and retinal pigment epithelium (RPE) and, as in the brain, also to compressive force by an overpressure. The significance of these biomechanical interactions has not yet been elucidated, but mechanical adaptation within the tissue has been recognized already during development where radial stretch inside the growing eye is enabled by an increased elastic modulus [2].

Several diseases of the retina have a mechanical background and are therefore suitable for studies of biomechanical impact on CNS tissue homeostasis. In rhegmatogenous retinal detachment (RRD), vitreous fluid enters the subretinal space through a rupture dislodging the retina from the retinal pigment epithelium (RPE) and detaching it into the vitreous space removing it from normal biomechanical influence [3-7].

The yearly incidence of the condition is approximately 1.4:10000 individuals, and the lifetime risk has been reported to be 1:300 [6,7]. In the majority of cases, patients suffer from rapid and profound vision loss progressing from the peripheral to central visual field. Reattachment is attained by surgically either by scleral buckling or vitrectomy, which positions and fixates the retina once again towards the RPE. Reattachment surgery has proven relatively effective in terms of anatomical repositioning of the retina and restoration of retinal function [3,4]. However, if the detachment includes the macula, permanent loss of visual acuity is seen within hours even if surgical attachment is attained [8]. Electrophysiological investigations of the recovery of retinal function after retinal detachment are not plentiful, however, it has been reported that the cone photoreceptor system does not recover as well as the rod system [3, 8]. Traditionally, this has been attributed to ischemia of macular cones due to an increased distance to the choroid. However, in other conditions where the macula is separated from the RPE/choroid, visual loss is often much less prominent, and the current ischemic paradigm may therefore be incomplete [9]. Support for this theory is also gained by the fact that, experimental detachment using viscoelastic fluid in large animals, appears to induce very little loss of retinal function in spite of several weeks of retinal detachment [10].

We have recently explored the relationship between the retinal biomechanics and retinal homeostasis. Using an in vitro model of adult porcine retina, we were able to show that adult retinal explants maintained in culture with no physical support collapse and display severe signs of neuronal degeneration and gliosis after 2 days in vitro [11]. In contrast, retinas in which tissue collapse is prevented by either stretching the tissue or supporting the inner retina, display excellent survival for at least 10 days [11,12]. These retinas show preservation of ultrastructural elements such as inner and outer segments, the outer limiting membrane, and synapses [12].

To further pursue the relationship between retinal biomechanics and tissue homeostasis, and its relevance for disease, we here have emulated the clinical RRD paradigm within the in vitro environment and explored the dynamics of early cellular events. We have thus constructed an in vitro model using adult porcine retinal explants in which tissue support is abolished and then reinstated mimicking the clinical situation of detachment and surgical reattachment, and we here report the progression of neuronal cell death and gliosis within this system.

MATERIAL AND METHODS

Tissue Culturing

All proceedings and animal treatment were in accordance with the guidelines and requirements of the government committee on animal experimentation at Lund University and with the ARVO statement on the use of animals in ophthalmic and vision research. The porcine eye was chosen as a model since it has a retina with similar overall cone/rod and ganglion cell distribution as the human counterpart [13,14]. Eyes were harvested from adult pigs aged between 4 - 6 months euthanized by an overdose of sodium pentobarbital, (Apoteket, Umeå, Sweden). The neuroretinas were removed and cultured using the method described previously [12]. To summarize, the eyes were enucleated immediately after sacrifice and immersed in CO2 –independent medium (Invitrogen, Paisley, UK) in a container that was kept on ice until dissection. The anterior segment was excised by a sharp incision in the pars plana and cut 360 degrees and the vitreous was removed in one piece by carefully pulling it from the eyecup using sterilized tissue paper. The neuroretinas were gently dissected free from the pigment epithelium with microforceps and the optic nerve head was cut using micro scissors. Each neuroretina was sectioned into 6 pieces, measuring approximately 7x8 mm and specimens were distributed among the 12 explant culture modality groups to avoid selection bias (Table 1). In total, 15 eyes from 8 animals were used, yielding 78 specimens for culture and 2 eyes serving as a normal adult in vivo controls. The time from euthanization until actual explantation was between 15 - 60 mins.

For baseline experiments, explants were cultured for either 3h (n=18) or 12h (n=18) using three different settings: 1) free-floating (Fig.1 top); 2) with the photoreceptors positioned against the culture membrane (Fig. 1 middle, standard protocol) or, 3) with the inner retina positioned against the culture membrane (Fig. 1 bottom, IRS: Inner Retina Support). Culture

wells with Millicell- PCF 0.4 μm culture plate inserts were used (Millipore, Billerica, MA, USA). For the detachment/reattachment model, specimens were kept free-floating for either 3 or 12h, after which they were explanted onto culture plate inserts with the photoreceptors facing the membrane (n=9 and n=6 respectively), or with the ILM facing the culture membrane (n=9 and n=6 respectively). After the free-floating period, the explants were kept for 48h (total culture time=51 and 60h). Twelve explants were kept free-floating without reattachment to the culture membrane (detachment model) for 51 (n=6) and 60h (n=6). For free-floating specimens, 4ml culture medium was used per culture. For the remaining cultures, 1,5 ml was used. The culture medium was DMEM/F12 (Invitrogen), supplemented with 10% fetal calf serum (Sigma-Aldrich, St Louis, MO, USA) as well as a cocktail containing 2 mM L-glutamine, 100 U/ml penicillin and 100 ng/ml streptomycin (Sigma Aldrich). The explants were maintained in an incubator at 37 °C at 95% humidity and 5% CO2. The medium was exchanged once after 48h of culture.

Histology

Histological examinations were performed as previously described by Taylor et al., 2014 [12], and only briefly recapped here. After culturing, the explants were fixed in 4% paraformaldehyde in 0.1M phosphate buffer, pH 7.2 for 2h in 4 °C. The normal adult in vivo controls were fixed immediately after harvest using the same paraformaldehyde concentration for 4h in 4 °C. The explants were then infiltrated with 0.1M Sörensens medium with increasing concentrations of sucrose up to 25%. They were then embedded in egg albumin/gelatine medium for cryosectioning at -20 °C with a section thickness of 12 μm. For light microscopy, every 10th slide was stained with hematoxylin and eosin. For immunohistochemical labeling, adjoining slides with sections originating from the center of the explants (the area centralis in the normal control) were chosen. The specimens were rinsed

3 times with PBS containing 0.1% Triton- X, and then incubated with PBS containing 0.1% Triton-X and 1% bovine serum albumin (BSA) for 20 minutes at room temperature. After this, the specimens were incubated overnight at 4 °C with the respective primary antibody (Table 2). In the double labeling for GS/bFGF, both primary antibodies were added at this stage. The specimens were then rinsed in PBS-Triton-X (0.1%), and incubated for 45 minutes with a secondary fluorescein isothiocyanate (FITC) or Texas Red-conjugated antibody (Table 1). In the double labeling for GS/bFGF, both secondary antibodies were added at this stage. The specimens were then mounted in hard-set Vectashield mounting medium with 4',6-diamidino-2-phenylindole (DAPI; Vector laboratories Inc., CA, USA). Negative control experiments were performed as above, replacing the primary antibody with PBS containing 0,1% Triton-X and 1% BSA. Normal porcine adult retina was used as a positive control. Normal control tissue and cultured specimens were processed in the same batch for each immunohistochemical labeling.

Microscopy and image analysis

The histological sections and immunohistochemically labeled specimens were examined using an using an optical and 293 epifluorescence microscope (Axio Imager M2, Carl 294 Zeiss Microscopy GmbH, Jena, Germany) equipped 295 with a digital camera system (AxioCam MRm, Carl 296 Zeiss) and a digital acquisition system (ZEN 2012 blue 297 edition, Carl Zeiss). Photographs were taken at each end of the section, and in the center. Images were viewed and processed using Photoshop (Adobe Systems, Mountain View, CA).

Statistical Analysis

Immunohistochemically labeled sections were used to statistically quantify survival of ganglion cells and cone photoreceptors as well as apoptosis. The intensity measurements and the cell counts were performed in a blinded manner, using a method previously described

[15]. Three central sections per cultured specimen were analyzed for NeuN, transducin, and TUNEL labeling, along with three sections per in vivo reference eye. In vivo reference tissue and cultured specimens were processed in the same batch for each immunohistochemical and TUNEL labeling. Three photographs were obtained from each section, and the number of labeled cells (NeuN, transducin) or mean fluorescence intensity (TUNEL) were counted/measured at 20x magnification. For TUNEL labeling intensity measurements, images were analyzed using ImageJ (Rasband, W.S., ImageJ, U. S. National Institutes of 306 Health, Bethesda, MD, http://imagej.nih.gov/ij/) as previously described [15]. A rectangular area of 770x780 (TUNEL) pixels was analyzed and the measurement included the entire inner-to-outer retinal areas except for inner and outer segments. From each image, the channels were separated, the background subtracted, and the mean fluorescence measurement was recorded. A representative image for the figure panels was chosen from each labeling batch. Data were analyzed using ANOVA with a Tukey post hoc test (GraphPad InStat; GraphPad Software, San Diego, CA). Raw data from cell counts and fluorescence measurements were used to generate mean values for each of the groups. Values of $p<0.05$ were considered significant.

RESULTS

Macroscopic observations

After explantation, the edges of the free-floating specimens almost immediately folded and the specimens subsequently rolled up with the inner retina facing inwards. In the detachment/reattachment groups, explants could readily be flattened against the culture membrane using careful manipulation with a curved forceps. Specimens that had been floating for 12 hours had become more tightly rolled up compared with 3-hour counterparts. In the detachment groups (free-floating for 51 or 60 hours) were found to be very tightly rolled up. All remaining specimens that had been placed against the culture membrane remained flat throughout the culture period with no apparent difference between groups.

In vivo controls

The overall morphology and immunohistochemical characteristics of the normal adult porcine retina have been well described previously but will be summarized here [11,12].

No TUNEL labeled cells were seen in the normal adult porcine retina (Fig. 2A). NeuN labeling showed a multitude of large cell bodies in the ganglion cell layer (GCL) corresponding to ganglion cells (Fig. 2B). The transducin antibody labeled cone photoreceptor nuclei in the outer part of the outer nuclear layer (ONL) with terminals in the outer plexiform layers (OPL) and inner and outer segments.(Fig. 2C). Rhodopsin immunohistochemistry revealed strong labeling of outer segments at the outer border of the specimen, as well as weaker labeling of inner segments (Fig. 2D). Specimens labeled with glial fibrillary acidic protein (GFAP) displayed strong labeling of astrocytes and Müller cell endfeet at the innermost part of the specimens and occasional thin vertical fibers in the inner retina (Fig. 2E).

Cultured explants

Apoptosis

Minimal TUNEL labeling, mainly in the outer part of the specimens, were seen in floating, standard as well as IRS (inner retinal support) baseline explants after 3 and 12 hours without any difference between the culture modality groups, or when compared to the in vivo controls (Figs. 3A-F and 4). Numerous labeled cells were present in all nuclear layers after 51 or 60 hours in free-floating and reattached standard explants with significantly higher overall labeling intensity cells present compared with reattached IRS counterparts (Figs. 3G - L and 4 A-B).

Ganglion cells

All three baseline groups displayed a statistically significant reduction of NeuN labeled ganglion cells to approximately 30-40% compared with in vivo controls after 3 hours in vitro without any difference between the culture modality groups (Figs. 5A - C and 6A, $p>0.001$). After 12 hours in vitro, significantly more NeuN labeled cells were present in IRS specimens compared with free-floating and standard cultured counterparts (Figs. 5D - F and 6B). In free-floating explants and in reattached standard specimens, very few NeuN labeled ganglion cells remained after 51 and 60 hours, and reattached IRS explants contained significantly more labeled cells at these time points (Figs. 5G - L and 6). Reattached IRS explants displayed no significant ganglion cell loss compared to baseline.

Cone and rod photoreceptors

A significant reduction in the number of transducin labeled cone photoreceptors was seen already at 3 hours in vitro in the three baseline culture modality groups, although the IRS and standard cultured groups retained a normal labeling pattern and cellular morphology, compared with in vivo controls, (Figs 7A - C and 8A, $p>0.001$). Free-floating specimens

displayed a disrupted ONL and a discontinuous OPL with very few inner and outer segments whereas standard and IRS counterparts had a morphology comparable to the in vivo controls. At 12 hours, this appearance was retained in IRS explants, whereas free-floating specimens displayed a disrupted cone morphology with significantly fewer labeled cells when compared with 3-hour free-floating as well as with 12-hour IRS counterparts (Figs. 7D, F and 8B). In standard cultured explants, the number of transducin labeled cones was the same as in IRS counterparts, but labeled cells as well as terminals in the OPL displayed a disrupted morphology and discontinuous labeling (Fig. 7E). Reattached IRS cultures retained a normal cone morphology at 51 hours (3+48) with some disruption of cells in the ONL at 60 hours (12+48) (Figs. 7I and L). Significantly fewer transducin labeled cones remained in free-floating and reattached standard cultured counterparts at these time points (Figs. 7H - I and 8). Reattached IRS explants displayed no significant cone photoreceptor loss compared to baseline, however there was significantly more transducin labeled cones in reattached IRS explants after 60 hours (12+48) compared with 12-hour free floating counterparts.

Rhodopsin labeled outer segments were found in all baseline modality groups after 3 or 12 hours of culture comparable to the in vivo controls (Figs. 9A - F). Inner segments were also seen and often weak labeling was present in the ONL. In 51-hour free-floating explants and in both groups of reattached counterparts (3+48 hours), the inner/outer segment area was thinner than in in vivo controls (Figs. 9G - I). More labeled structures in this area could be seen in IRS specimens compared with free-floating and reattached standard cultured counterparts. After 60 hours of culture, all groups displayed disorganized labeled structures in the outer/inner segment area with mild to moderate labeling of the entire ONL, a phenomenon well known to be associated with photoreceptor degeneration (Figs. 9J-L).

Müller cell activation

GFAP labeling of baseline explants cultured for 3 or 12 hours revealed no certain difference compared with in vivo controls with labeling in horizontal fibers in the innermost retina and occasional vertical structures extending into the retinal layers (Figs. 10A-F). In 51- and 60-hour specimens, free-floating and reattached standard explants displayed profound upregulation of labeling in vertical Müller cell fibers traversing all retinal layers (Figs. 10G, H, J, and K). Reattached IRS counterparts also displayed GFAP upregulation compared with in vivo controls in vertical Müller cell fibers, but these fibers were thinner, less intensely labeled, and did not traverse the ONL (Figs. 10I and L).

DISCUSSION

In this paper, we have studied modulation of the biomechanical environment in an in vitro model of retinal rhegmatogenous detachment (RRD). The hypothesis being that tissue support may in fact be an important factor for tissue homeostasis before and after treatment of the condition. Within our culture setting, the medium represents the nutritionally supportive aqueous and vitreous fluids in vivo and the tissue support provided by the membrane, the physical forces that influence the retina within the living eye. Placing the explanted retina with its inner border against the culture membrane provides firm tissue support which in our model represents the attached retina in vivo [12], whereas free-floating counterparts simulates the clinical condition in which the detached retina floats in the vitreous space without support from the surrounding tissues. This in vitro setup offers substantial control not only over the physical forces acting on the tissue, but also the chemical composition of the medium, as well as exact timing of interventions. The dynamics of cellular events related to biomechanics can thus be studied under standardized conditions with a precision that is difficult to obtain in vivo.

Within the model, the detached retina without tissue support (free-floating) displays progressive gliosis and apoptotic cell death in all nuclear layers with almost no surviving ganglion cells and cone photoreceptors after 60 hours in vitro. These findings are well in line with pathologic reactions reported in human eyes with advanced RRD [16,17]. In contrast to cones, rod photoreceptors in our model appear to be more resistant to the in vitro detachment evident by a substantial amount of surviving rhodopsin labeled cells even after 60 hours of detachment which is in accordance with previous clinical and experimental studies in vivo [5,18]. To compare these results with the literature regarding experimental detachment in vivo is not straightforward, since pathologic reactions to detachment, such as glial reactivity,

shows great variability between species and even strains [19,20]. The most commonly used method involving subretinal injection of viscoelastics, in the porcine eye, produces Müller cell reactions, whereas effects on retinal neurons are more uncertain [10,21].

In the retina, the biochemical and biomechanical homeostasis is maintained by Müller cells, which can alter their physical properties through up- or downregulation of intermediary filaments (such as GFAP and vimentin) [11,12,22,23]. This allows Müller cells to control the tissue-wide as well as the cellular biomechanical environment [11,12,22,23]. In this setting, it is interesting to note that the stiff, intermediary filament-rich Müller cell endfeet contain mechanosensory cation channels, such as TRPV4, which are known to respond to changes in cell membrane stretch through Ca2+ influx [11,12,22-24]. Influx of Ca2+ is a known trigger of intermediary filament upregulation in Müller cells [12,25,26]. A link between TRPV4 an intermediary filament upregulation remains to be elucidated, however, it has been suggested that this system may provide the retina with a mechanism of sensing and responding to biomechanical changes [10, 24].

During retinal insult or disease, Müller cells become reactive, a process which, if left untreated, may lead to gliosis. We and others have previously shown that gliosis, characterized by upregulation of GFAP in Müller cells, lead to a loss of normal homeostatic functions, creating a neurotoxic environment which accelerates cell death [11,12, 25-27]. This phenomenon is highly pronounced in standard cultured explants kept for long time periods, up to 10 DIV, at which time mostly gliotic glial cells remain [12]. In contrast, long term IRS cultures display no signs of gliosis [12]. In accordance, free-floating and reattached standard cultures in the current experiments displayed an increased expression of GFAP in disorganized Müller cell fibers spanning the entire retina, whereas reattached IRS specimens

showed only minimal labeling of Müller cell processes in the inner layers, indicating a hampered glial response in explants receiving physical support.

Perhaps the most important and novel finding of our study is that ganglion cell and cone photoreceptor degeneration can be impeded and overall apoptosis as well as gliosis attenuated if the retina is reattached with reinstated tissue support after a period of detachment. In fact, when analyzing cone photoreceptors survival, significantly more transducin labeled cells were found in reattached IRS explants after 60 hours compared with detached counterparts at 12 hours. This indicates that restoration of tissue support not only arrests neuronal cell death, but that injured cells can be restored to health by this intervention.

Retinal detachment has been explored in vitro previously [28], but to our knowledge the present work represents the first example in which reattachment has been performed and showed to arrest pathological events in a manner emulating clinical detachment and surgical reattachment. Using this model, we for the first time have shown that lack of tissue support may be an important instigator of RRD pathology, and that its restitution may at least be partially responsible for treatment effects seen clinically. These results reinforce the relationship between the biomechanical environment and retinal homeostasis, and strengthens the concept of clinical reattachment emulation within the in vitro environment.

The phenomenon of neuronal rescue is of particular interest when the early and profound loss of ganglion cells is considered with only 30 - 40% of cells remaining after 3 hours in vitro regardless of culture modality. In contrast to permanently detached, or reattached standard explants, ganglion cell death did not progress in 12-hour baseline or in reattached IRS explants (51 and 60 hours). We have previously reported approximately the same amount of reduction of ganglion cells in IRS cultures after 5 days in vitro [12], and when these results are put together, we can now draw two conclusions. First, a very early event associated with

the explantation procedure, initiates ganglion cell death, and second, this process is halted in explants placed with the inner retina against the culture membrane. One possible mechanism of initial trauma is ischemia since there was a delay of 15 - 60 minutes between sacrifice of the animal until actual explantation. Ganglion cell loss however, was more profound compared with initial loss of photoreceptors indicating an event specifically affecting these cells. The explantation process inevitably includes axotomy of ganglion cell axons which is well known to produce ganglion cell death [29,30]. Significant loss of ganglion cells after optic nerve transections does not occur until two - three days after the trauma [31], however, the axotomy trauma involved in the explantation procedure is two-fold. First, the axons of the optic nerve is transected at enucleation, and second, intraretinal ganglion cell axons are cut when the explanted retinal piece is retrieved. We cannot rule out the possibility of explantation related axotomy as at least partly responsible for the dramatic decrease of NeuN positive ganglion cells already at 3 hours of culture, however, the fact that surviving cells are rescued only in the reattached IRS explants after this time suggests that the biomechanical environment with restoration of tissue support is of significant importance for ganglion cell survival after detachment.

Our study does not provide the exact mechanism through which the lack of tissue support induces detrimental effects on retinal homeostasis but our results suggests a mechanism of biomechanical sensing/responding with a link to biochemical homeostasis. Interestingly, the inner retina contains mechanoreceptors (TRPV4) in ganglion cells as well as Müller cell end-feet reinforcing the notion that this region is in fact the center of retinal biomechanical control [24]. The elastic retina is stretched against the RPE and choroid during development, and we hypothesize that this state is maintained in the adult eye by retina - RPE adhesion in combination with the intraocular pressure within the closed eye [2, 32]. In accordance with

this theory, Jackson and colleagues noted undulation of the inner limiting membrane (ILM) immediately after retinal detachment in a porcine experimental model which in contrast to most other models using subretinal viscoelastic, more closely resembles the clinical condition in which the retina detaches as a result of a peripheral rupture [33]. The sudden loss of adhesive and hydrostatic forces acting on the detached retina in this setting thus may induce collapse of the elastic tissue. In accordance, we here saw that free-floating explants without any support from the culture membrane quickly became rolled up with the inner retina facing the center and outer retina on the outside. We have previously reported that the ILM of IRS explants is flat and well apposed to the culture membrane and that these cultures show significant attenuation of neuronal cell death and gliosis compared with standard cultured counterparts for up to 10 days [12]. In addition, standard cultures show similar attenuation of pathological reactions if they are stretched in a manner emulating the state found within the living eye [11]. To sum up our findings and provide a comprehensive theory related to clinical RRD, the elastic retina collapses as a result of disruption of its biomechanical environment when removed from its entoptic location within the living eye. This collapse can be counteracted by mechanical stabilization, which resets the biomechanical state of the tissue and restores homeostasis. Our results reinforce the notion of a strong relationship between the biomechanical environment and homeostasis within the retina which has significant bearing on pathologic events related to RRD, and may also have impact on other regions within the CNS under biomechanical influence.

FIGURE LEGENDS

Figure 1. Illustration of the ”Retinal detachment in a box” concept. Retinal explants are kept free-floating in culture medium corresponding to the detached retina in vivo. After 3 or 12 hours of detachment, explants were either kept detached (Float), reattached with photoreceptors facing the culture membrane (Standard) or reattached with the inner retina facing the membrane (IRS: inner retinal support) and then kept in culture for an additional 48 hours.

Figure 2. Immunohistochemical labeling of normal adult porcine retina in vivo. DAPI counterstaining (blue) to identify neuronal layers was performed on D and E. A. No TUNEL labeled cells are present within the retinal layers. B. NeuN labeling of ganglion cells displays numerous labeled cells of ganglion cell morphology in the GCL. C. Transducin labeling shows well labeled cone photoreceptor nuclei in the outer part of the ONL with terminals in the OPL and inner and outer segments. Weak labeling is also present in the INL. D. Rhodopsin labeling of rod photoreceptors shows strong labeling in the rod outer segments, with weaker labeling present in the inner segments and rod photoreceptor nuclei. E. GFAP labeling shows thin vertical Müller cell fibers, mainly in the inner part of the specimen. Strong labeling of horizontal fibers and astrocytes in the NFL is also seen. GCL = ganglion cell layer; INL = inner nuclear layer; OPL = outer plexiform layer; ONL = outer nuclear layer. IS = inner segments; OS = outer segments. Scale bar: 50 μm.

Figure 3. TUNEL labeling. In free-floating, Standard, and IRS (inner retinal support) specimens, minimal labeling is present in the outer part after 3 or 12 hours in culture (A-F). In free-floating explants and in retinas that have been placed with photoreceptors apposed to the culture membrane after 3 or 12 hours of free-floating, numerous labeled cells are present throughout the nuclear layers after a total culture time of 51 and 60 hours (G, H, J and K).

Significantly fewer labeled cells are present in IRS counterparts (I and L). GCL = ganglion cell layer. INL = inner nuclear layer; ONL = outer nuclear layer. Scale bar: 50 μm.

Figure 4. Statistical analysis of TUNEL labeling intensity measurements. A. 3h baseline, 51h free-floating and 3h+48h detachment-reattachment explants. B. 12h baseline, 60h free-floating and 12h+48h detachment-reattachment explants. Minimal TUNEL labeling was found baseline explants after 3 and 12 hours, with no significant difference between the culture modality groups. 51h free-floating and IRS and ST detachment-reattachment explants displayed a significant increase TUNEL labeled cells from baseline. 51h free-floating explants showed a significantly higher number of labeled cells compared to the 3h detachment + 48h IRS reattachment group ($p<0.001$). After 60h, free-floating and 12h+48h ST explants revealed a significant increase in TUNEL labeling compared to baseline, and a significantly higher level of labeling compared to 12h+48h IRS specimens ($p<0.001$ and $p<0.001$ respectively). Error bars SEM.

Figure 5. NeuN labeling. In free-floating specimens (A, D, G and J), progressively fewer ganglion cells are labeled over time. The same pattern is evident in standard cultures (B and E) and in reattached standard cultures (H and K). In all IRS counterparts, significantly more ganglion cells are labeled. GCL = ganglion cell layer. Scale bar: 50 μm.

Figure 6. Statistical analysis of cell counts of NeuN-labeled ganglion cells. A. 3h baseline, 51h free-floating and 3h+48h detachment-reattachment explants. B. 12h baseline, 60h free-floating and 12h+48h detachment-reattachment explants. All three 3h baseline explants displayed a statistically significant reduction of NeuN labeled ganglion cells to approximately 30-40% compared with in vivo controls. After 12 hours in vitro, significantly more NeuN labeled cells were present in IRS specimens compared with free-floating and standard cultured counterparts ($p<0.001$ and $p<0.001$ respectively). After 51 and 60 hours, reattached

IRS explants contained significantly more labeled cells compared to free-floating and standard counterparts ($p<0.001$ for all comparisons). Reattached IRS explants displayed no significant ganglion cell loss compared to baseline at both time points. Error bars SEM.

Figure 7. Transducin labeling. Free-floating explants display progressively fewer labeled cone nuclei in the outer part of the ONL and a disrupted OPL (A, D, G, J). The same is true for standard cultured explants after 12 hours, and in reattached standard explants (E, H, K). In contrast, IRS explants display an almost normal number of cones with normal organization after 3 and 12 hours (C and F). This is also true for reattached IRS explants that have been free-floating for 3 hours (I). In 12+48 hour counterparts (L), the number of labeled cones are still almost normal, but their organization in the ONL is disrupted. OPL = outer plexiform layer; ONL = outer nuclear layer; IS/OS = inner and outer segments. Scale bar: 50 µm.

Figure 8. Statistical analysis of cell counts of Transducin-labeled cells. A. 3h baseline, 51h free-floating and 3h+48h detachment-reattachment explants. B. 12h baseline, 60h free-floating and 12h+48h detachment-reattachment explants. No significant change was found in the number of transducin labeled cone photoreceptors in the 3h baseline cultures. After 12 hours, free-floating baseline specimens significantly fewer labeled cells when compared with 3-hour free-floating as well as with 12-hour IRS counterparts ($p<0.001$ for both comparisons). After both 51h and 60h, reattached IRS cultures displayed no significant cone photoreceptor loss compared to baseline, and a significant preservation of cells compared to free-floating and reattached St counterparts ($p<0.001$ for all comparisons). Error bars SEM.

Figure 9. Rhodopsin (green) and DAPI (blue) labeling. Rhodopsin labeled inner and outer segments can be seen in all groups after 3 or 12 hours of culture (A - F). Weak labeling is present in the ONL in free-Floating and IRS specimens. After 51 hours of culture, all groups

display shortened disrupted structures in the IS/OS area (G - I). After 60 hours of culture, all groups display disorganized labeled structures in the outer/inner segment area with mild moderate labeling of the entire ONL (J - L). ONL = outer nuclear layer, IS = inner segments, OS = outer segments. Scale bar: 50 μm.

Figure 10. GFAP (green) and DAPI (blue) labeling. Explants cultured for 3 or 12 hours display GFAP labeling in horizontal fibers in the innermost retina with occasional vertical structures extending into the retinal layers (A - F). Explants cultured for 50 or 61 hours display a strong upregulation of GFAP in vertical Müller cell fibers traversing the retinal layers (G - L). Free-Floating as well as reattached standard cultures display stronger and more widespread labeling compared to reattached IRS counterparts. ONL = outer nuclear layer. Scale bar: 50 μm.

CONFLICT OF INTEREST

All authors certify that they have NO affiliations with or involvement in any organization or entity with any financial interest (such as honoraria; educational grants; participation in speakers' bureaus; membership, employment, consultancies, stock ownership, or other equity interest; and expert testimony or patent-licensing arrangements), or non-financial interest (such as personal or professional relationships, affiliations, knowledge or beliefs) in the subject matter or materials discussed in this manuscript.

ACKNOWLEDGEMENTS

The authors would like to thank Elise Markström, Erica Cumléus and Oscar Manouchehrian for excellent technical assistance.

FUNDING

The following funding agencies and trusts provided financial support for the research included in this paper: The Faculty of Medicine, University of Lund, The Swedish Research Council, The Carmen and Bertil Regnér Foundation, The King Gustaf V and Queen Victoria Freemason Foundation, The Foundation of Debilitating Eye Diseases in Malmöhus County. The sponsors had no role in the design or conduct of this research.

ANIMAL EXPERIMENTS

All applicable international, national, and/or institutional guidelines for the care and use of animals were followed. All procedures performed in studies involving animals were in accordance with the ethical standards of the institution or practice at which the studies were conducted and with the ARVO statement on the use of animals in ophthalmic and vision research. This article does not contain any studies with human participants performed by any of the authors.

REFERENCES

1. DuFort CC, Paszek MJ, Weaver VM (2011) Balancing forces: architectural control of mechanotransduction. Nat Rev Mol Cell Biol 12(5):308-19.

2. Reichenbach A et al., (1991) Development of the rabbit retina. IV. Tissue tensility and elasticity in dependence on topographic specializations. Exp Eye Res. 53(2):241-51.

3. Schatz P, Holm K, Andreasson S (2007) Retinal function after scleral buckling for recent onset rhegmatogenous retinal detachment: assessment with electroretinography and optical coherence tomography. Retina 27:30-6.

4. Schwartz SG, Flynn HW Jr, Mieler WF (2013) Update on retinal detachment surgery. Curr Opin Ophthalmol 24(3):255-61.

5. Gong Y, Wu X, Sun X, Zhang X, Zhu P (2008) Electroretinogram changes after scleral buckling surgery of retinal detachment. Doc Ophthalmol. 117(2):103-9.

6. Algvere PV, Jahnberg P, Textorius O (1999) The Swedish Retinal Detachment Register. I. A database for epidemiological and clinical studies. Graefes Arch Clin Exp Ophthalmol. 237(2):137-44.

7. Haimann MH, Burton TC, Brown CK (1982) Epidemiology of retinal detachment. Arch Ophthalmol. 100(2):289-92.

8. Johansson K, Malmsjö M, Ghosh F (2006) Tailored Vitrectomy and Laser Photocoagulation Without Scleral Buckling for Primary Rhegmatogenous Retinal Detachment. Br J Ophthalmol 90:1286-91.

9. Wang M, Munch IC, Hasler PW, Prünte C, Larsen M (2008) Central serous chorioretinopathy. Acta Ophthalmol 86(2):126-45.

10. Sørensen NF et al., (2012) The effect of subretinal viscoelastics on the porcine retinal function. Graefe's Arch Clin Exp Ophthalmol. 250:79-86.

11. Taylor L, Moran D, Arnér K, Warrant E, Ghosh F (2013) Stretch To see - Lateral tension strongly determines cell survival in long-term cultures of adult porcine retina. Invest Ophthalmol Vis Sci 54:1845-56.

12. Taylor L, Arnér K, Holmgren Taylor I, Ghosh F (2014) Feet on the ground: Physical support of the inner retina is a strong determinant for cell survival and structural preservation in vitro. Invest Ophthalmol Vis Sci 55:2200-13.

13. Chandler MJ, Smith PJ, Samuelson DA, MacKay EO (1999) Photoreceptor density of the domestic pig retina. Vet Ophthalmol 2:179-184.

14.García M, Ruiz-Ederra J, Hernández-Barbáchano H, Vecino E (2005) Topography of pig retinal ganglion cells. J Comp Neurol 486(4):361-72.

15.Manouchehrian O, Arnér K, Deierborg T, Taylor L (2015) Who let the dogs out?: detrimental role of Galectin-3 in hypoperfusion-induced retinal degeneration. J Neuroinflammation 12:92.

16.Ghosh F, Johansson K (2012) Neuronal and Glial Alterations in Complex Long-Term Rhegmatogenous Retinal Detachment. Curr Eye Res 37:704-11.

17.Pastor JC et al., (2006) Intraretinal immunohistochemistry findings in proliferative vitreoretinopathy with retinal shortening. Ophthalmic Res 38(4):193-200.

18.Rex TS et al., (2002) A survey of molecular expression by photoreceptors after experimental retinal detachment. Invest Ophthalmol Vis Sci 43(4):1234-47.

19.Fisher SK, Lewis GP, Linberg KA, Verardo MR (2005) Cellular remodeling in mammalian retina: results from studies of experimental retinal detachment. Prog Retin Eye Res 24:395-431.

20.Matsumoto H et al., (2014) Strain difference in photoreceptor cell death after retinal detachment in mice. Invest Ophthalmol Vis Sci 22;55(7):4165-74.

21.Iandiev I et al., (2006) Glial cell reactivity in a porcine model of retinal detachment. Invest Ophthalmol Vis Sci 47:2161-71.

22.Lu YB et al., (2006) Viscoelastic properties of individual glial cells and neurons in the CNS. Proc Natl Acad Sci U S A. 103:17759–17764.

23.Lu YB et al., (2011) Reactive glial cells: increased stiffness correlates with increased intermediate filament expression. FASEB J. 25:624–631

24.Ryskamp DA et al., (2011) The polymodal ion channel transient receptor potential vanilloid 4 modulates calcium flux, spiking rate, and apoptosis of mouse retinal ganglion cells. J Neurosci 31(19):7089-101.

25.Bringmann A et al., (2006) Müller cells in the healthy and diseased retina. Prog Retin Eye Res. 25:397– 424.

26.Bringmann A et al., (2009) Cellular signaling and factors involved in Müller cell gliosis: neuroprotective and detrimental effects. Prog Retin Eye Res. 28(6):423-51.

27.Taylor L, Arnér K, Ghosh F. (2015) First Responders: Dynamics of Pre-Gliotic Müller Cell Responses in The Isolated Adult Rat Retina. Curr Eye Res. 40(12):1245-60.

28.Fontainhas AM, Townes-Anderson E (2011) RhoA inactivation prevents photoreceptor axon retraction in an in vitro model of acute retinal detachment. Invest Ophthalmol Vis Sci 52(1):579-87.

29.Komaromy AM et al., (2003) Long-term effect of retinal ganglion cell axotomy on the histomorphometry of other cells in the porcine retina. J Glaucoma 12:307-15.

30.Mey J, Thanos S (1993) Intravitreal injections of neurotrophic factors support the survival of axotomized retinal ganglion cells in adult rats in vivo. Brain Res 602:304-17.

31.Watanabe M, Fukuda Y (2002) Survival and axonal regeneration of retinal ganglion cells in adult cats. Prog Retin Eye Res 21(6):529-53.

32.Yao XY, Hageman GS, Marmor MF (1994) Retinal adhesiveness in the monkey. Invest Ophthalmol Vis Sci 35(2):744-8.

33.Jackson TL et al., (2003) An experimental model of rhegmatogenous retinal detachment: surgical results and glial cell response. Invest Ophthalmol Vis Sci 44:4026-34.

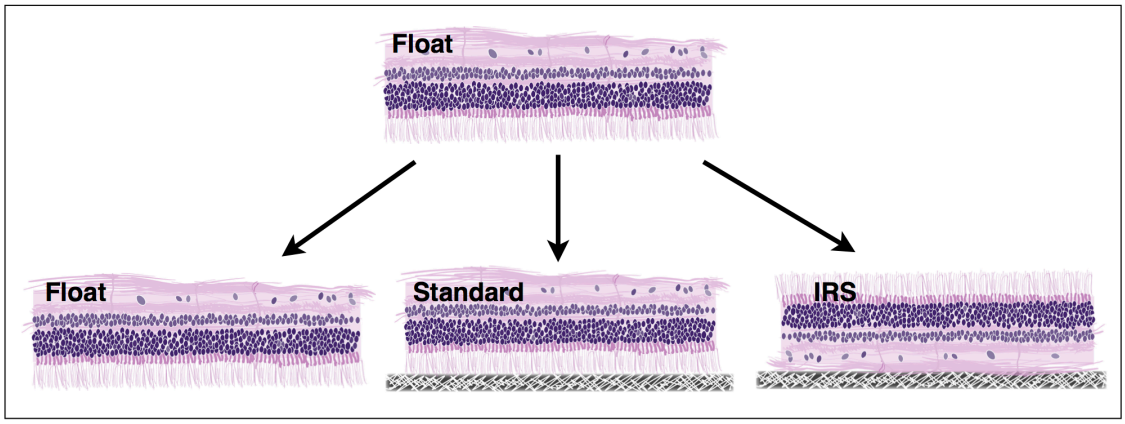

Figure 1.

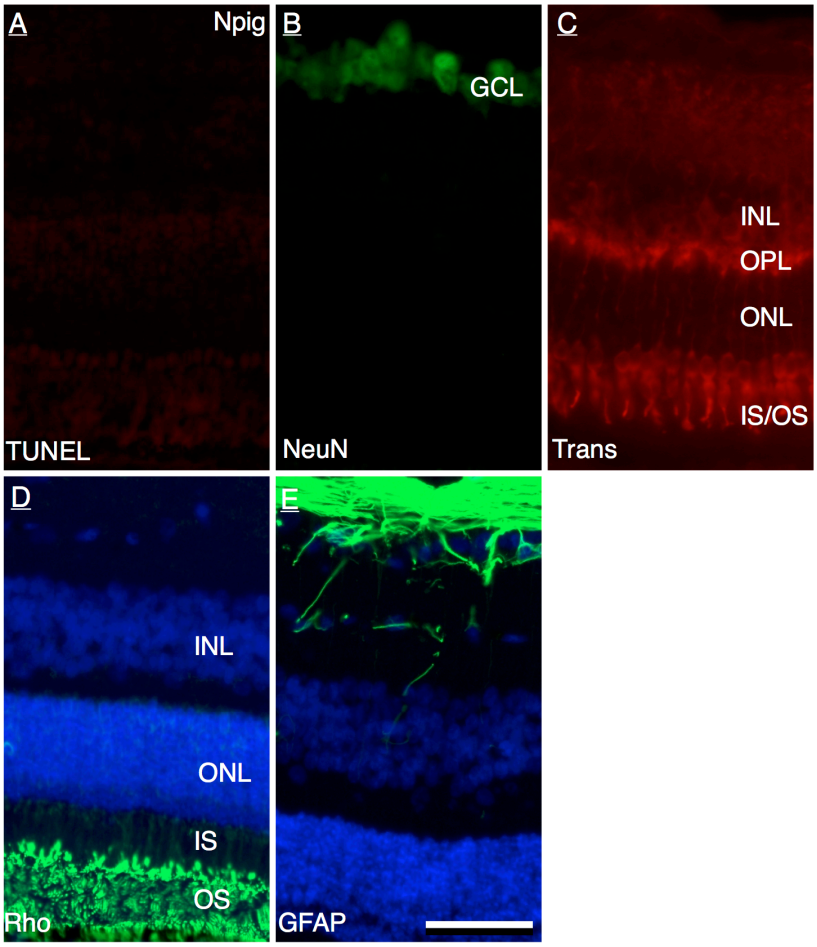
A
Npig
TUNEL
B
GCL
NeuN
C
INL
OPL
ONL
IS/OS
Trans
D
INL
ONL
IS
OS
Rho
E
GFAP

Figure 2.

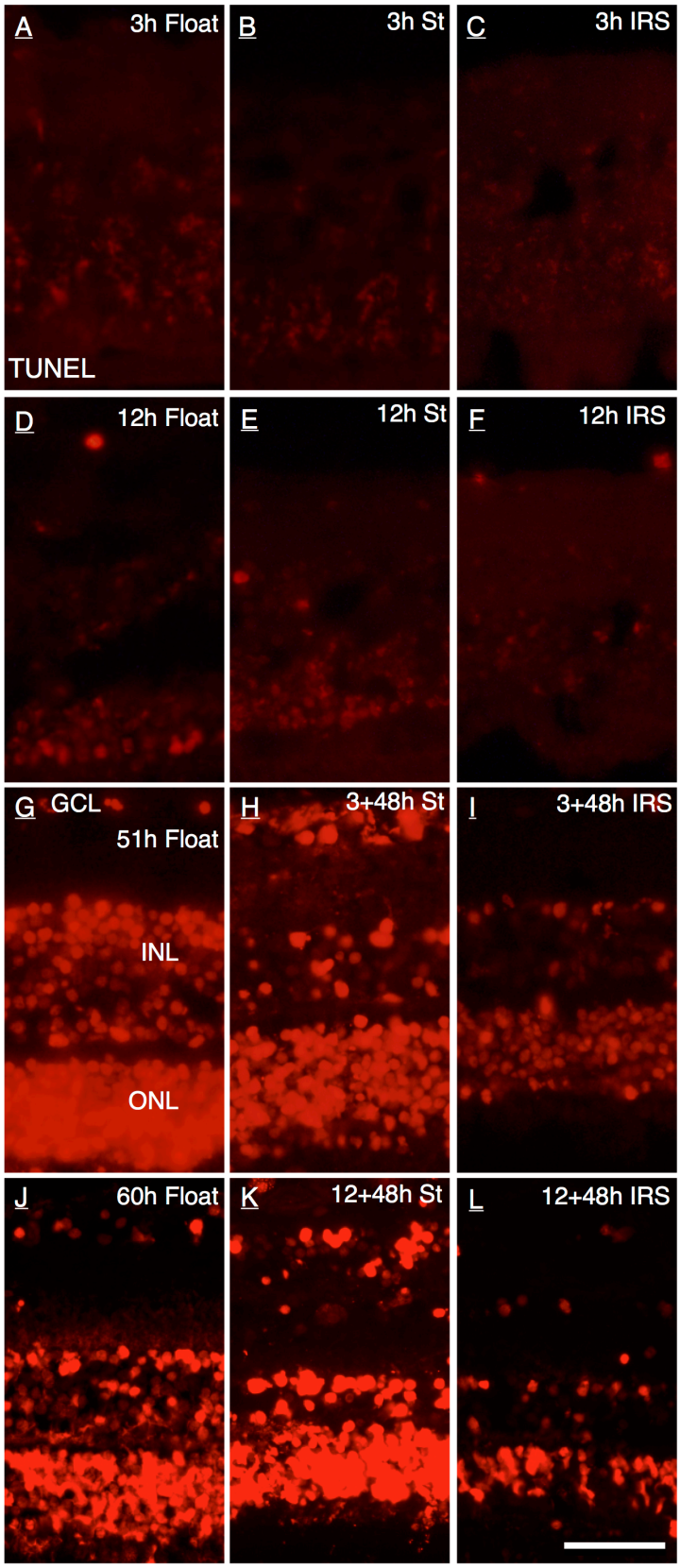
A
3h Float
B
3h St
C
3h IRS
TUNEL
D
12h Float
E
12h St
F
12h IRS
G
GCL
51h Float
INL
ONL
H
3+48h St
I
3+48h IRS
J
60h Float
K
12+48h St
L
12+48h IRS

Figure 3.

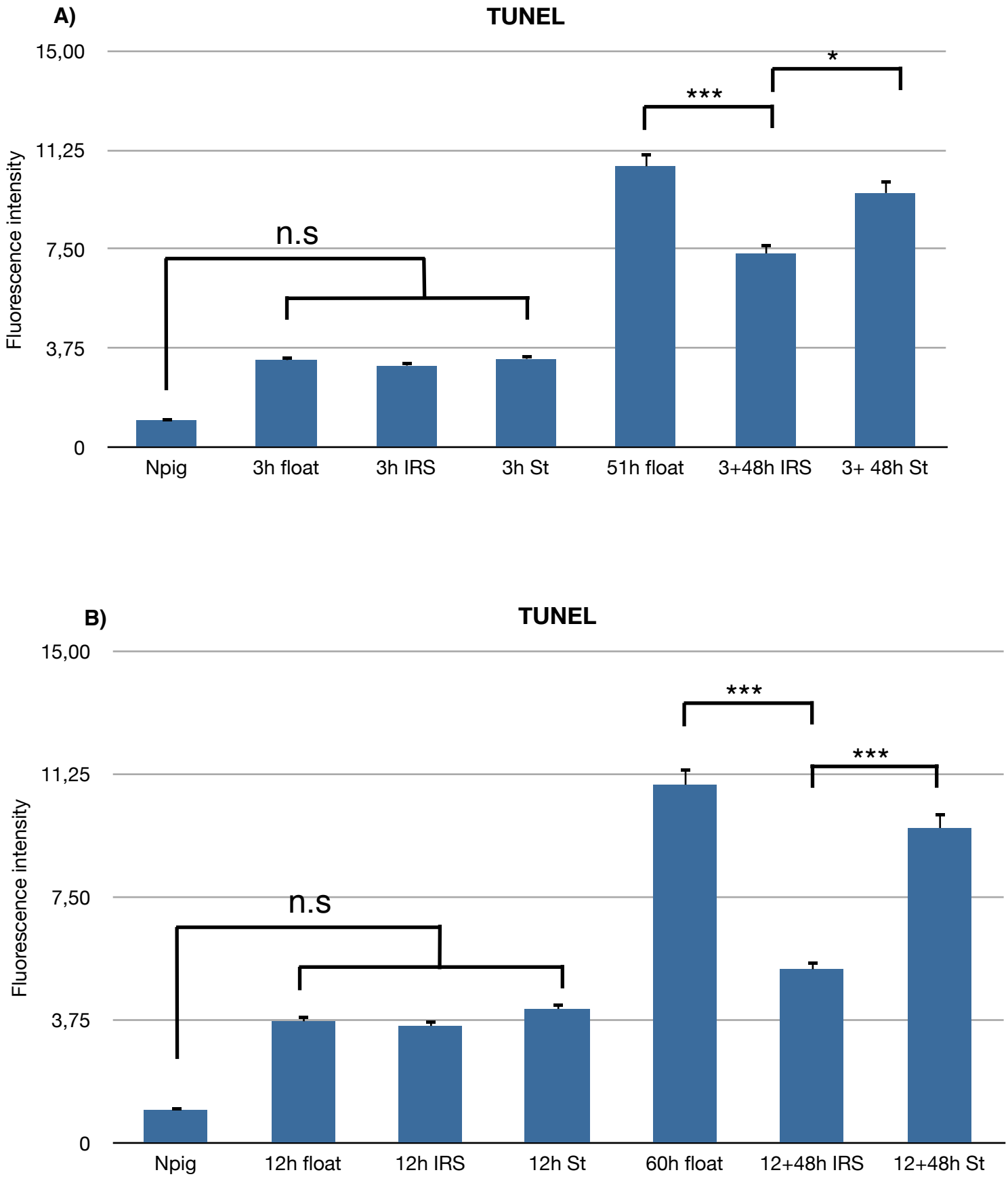
A)
TUNEL
15,00
11,25
7,50
3,75
0
Fluorescence intensity
n.s
***
*
Npig
3h float
3h IRS
3h St
51h float
3+48h IRS
3+ 48h St
B)
TUNEL
15,00
11,25
7,50
3,75
0
Fluorescence intensity
n.s
***
***
Npig
12h float
12h IRS
12h St
60h float
12+48h IRS
12+48h St

Figure 4.

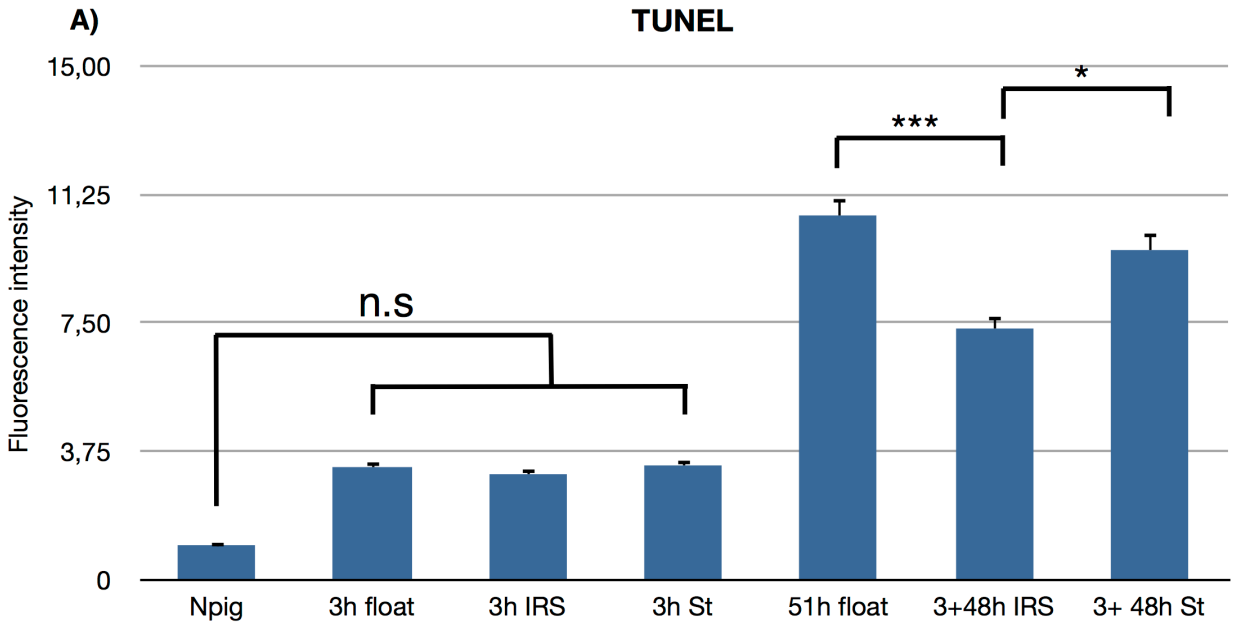
A)
TUNEL
15,00
11,25
7,50
3,75
0
Fluorescence intensity
n.s
***
*
Npig
3h float
3h IRS
3h St
51h float
3+48h IRS
3+ 48h St

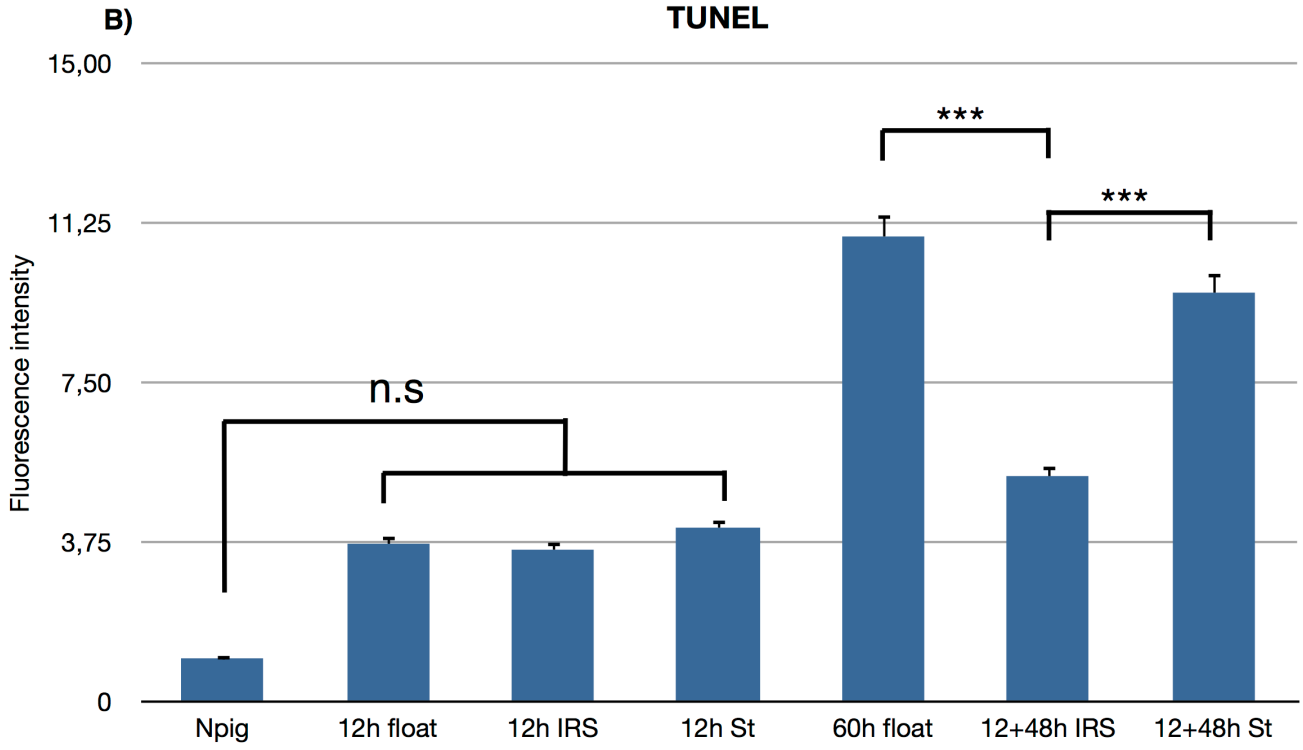
B)
TUNEL
15,00
11,25
7,50
3,75
0
Fluorescence intensity
n.s
***
***
Npig
12h float
12h IRS
12h St
60h float
12+48h IRS
12+48h St

Figure 4.

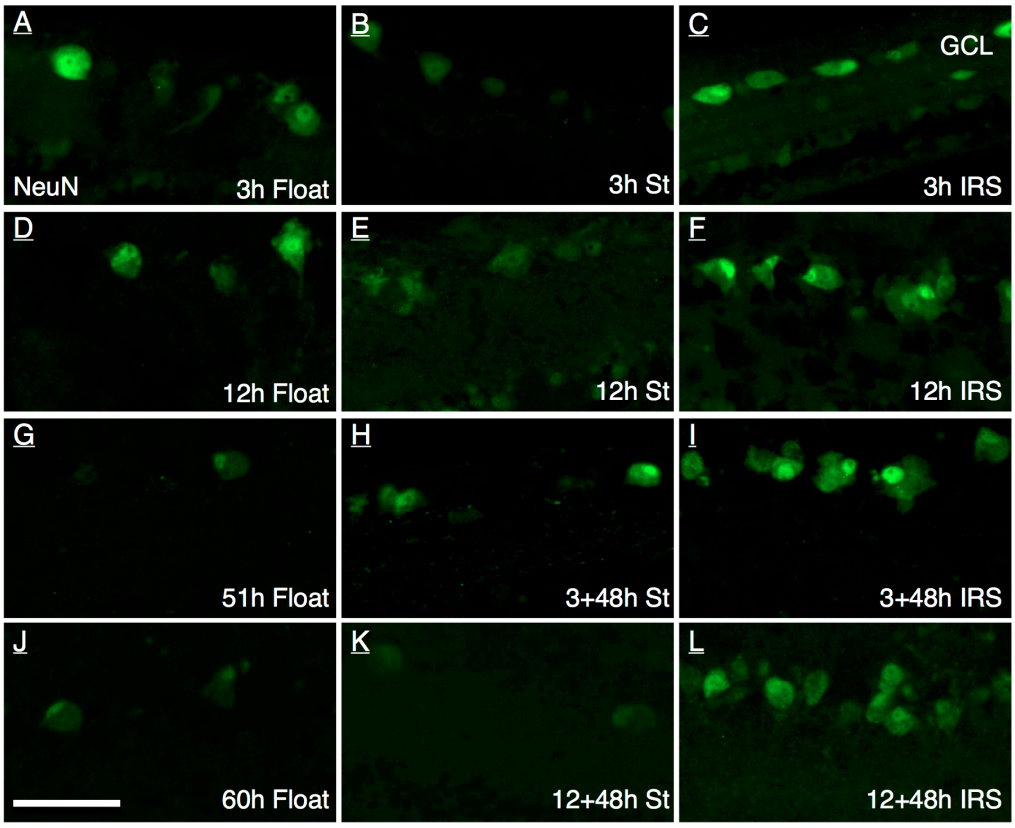
A
NeuN
3h Float
B
3h St
C
GCL
3h IRS
D
12h Float
E
12h St
F
12h IRS
G
51h Float
H
3+48h St
I
3+48h IRS
J
60h Float
K
12+48h St
L
12+48h IRS

Figure 5.

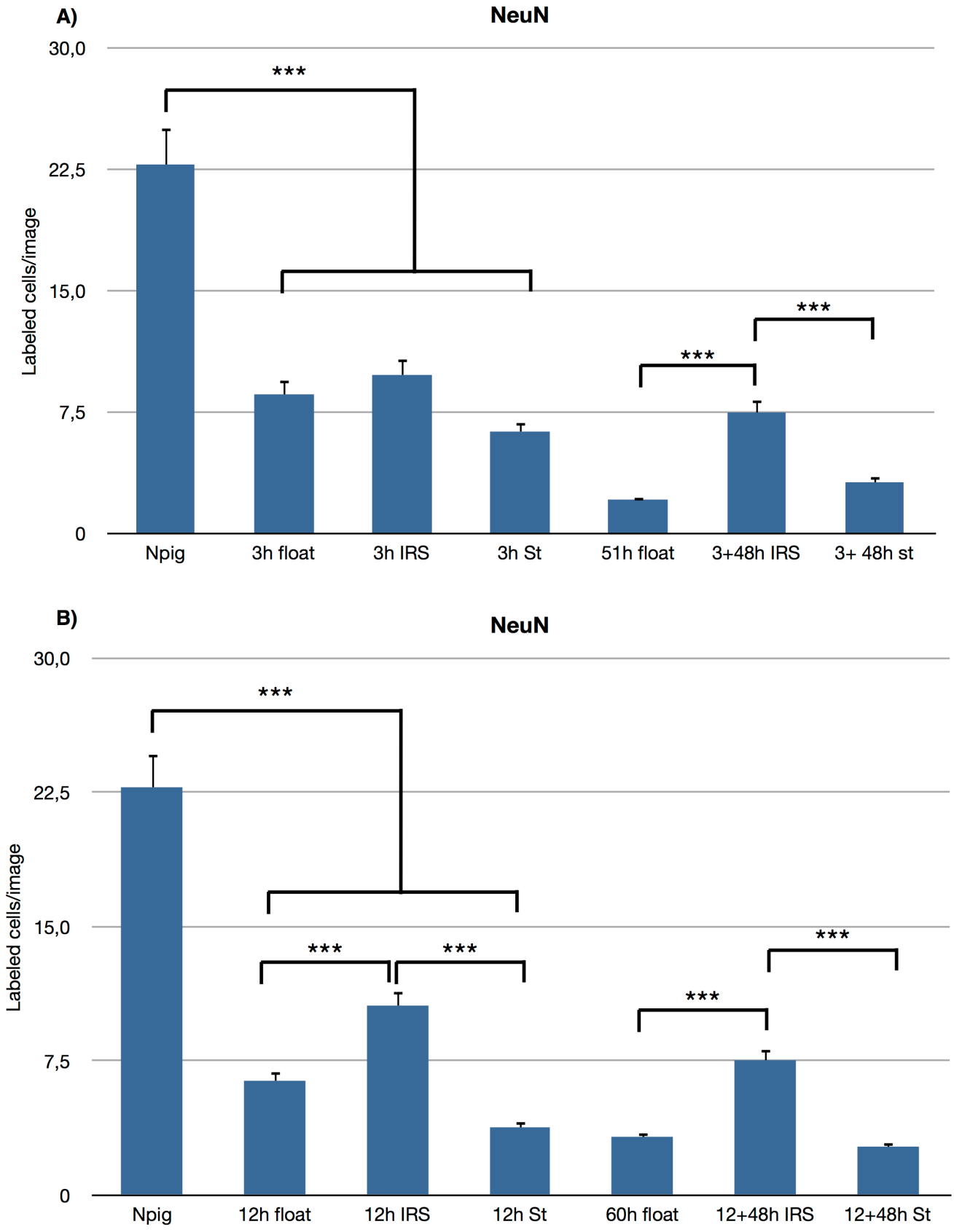
A)
NeuN
30,0
22,5
15,0
7,5
0
Labeled cells/image
***
***
***
Npig
3h float
3h IRS
3h St
51h float
3+48h IRS
3+ 48h st
B)
NeuN
30,0
22,5
15,0
7,5
0
Labeled cells/image
***
***
***
***
***
Npig
12h float
12h IRS
12h St
60h float
12+48h IRS
12+48h St

Figure 6.

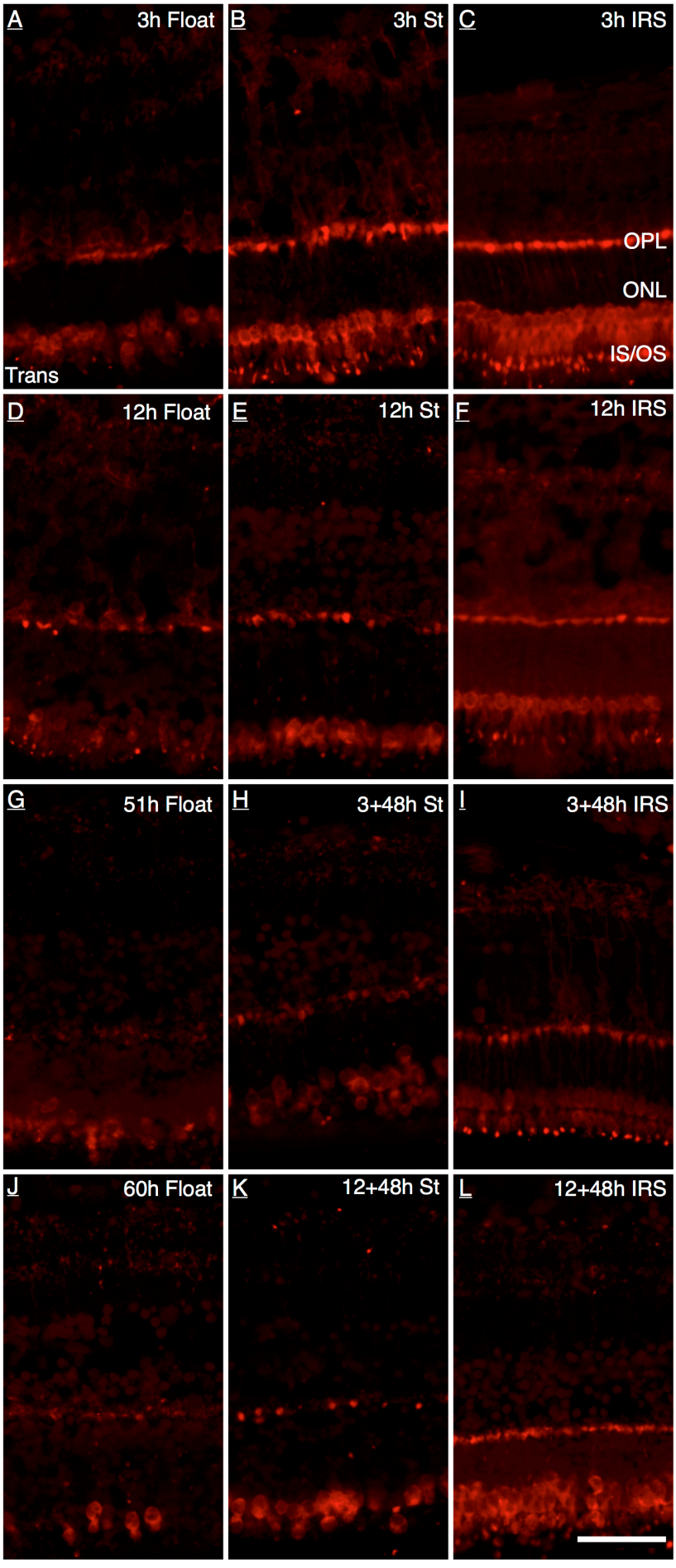
A
3h Float
B
3h St
C
3h IRS
OPL
ONL
IS/OS
Trans
D
12h Float
E
12h St
F
12h IRS
G
51h Float
H
3+48h St
I
3+48h IRS
J
60h Float
K
12+48h St
L
12+48h IRS

Figure 7.

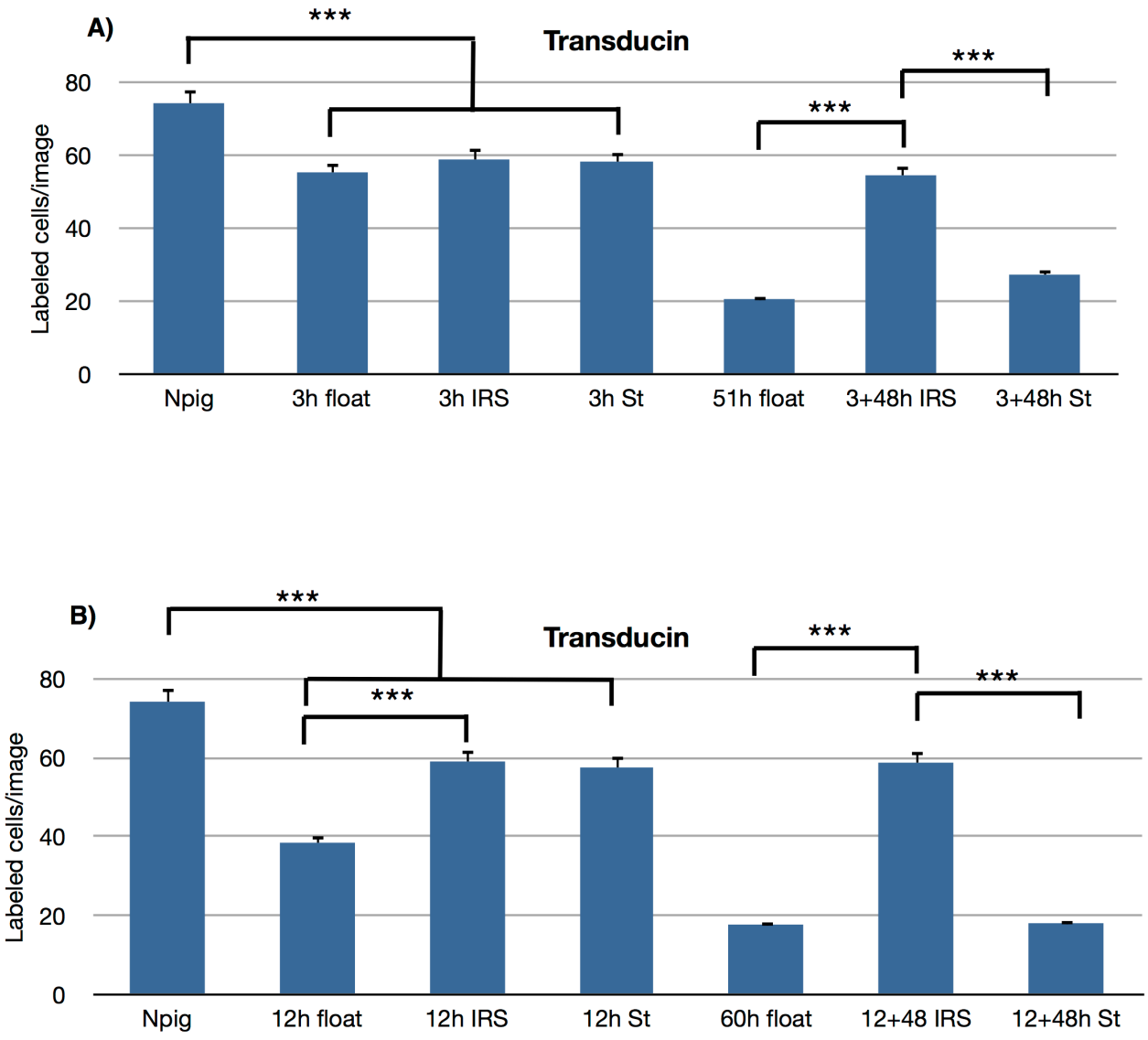
A)
Transducin
***
***
***
Labeled cells/image
0
20
40
60
80
Npig
3h float
3h IRS
3h St
51h float
3+48h IRS
3+48h St
B)
Transducin
***
***
***
***
Labeled cells/image
0
20
40
60
80
Npig
12h float
12h IRS
12h St
60h float
12+48 IRS
12+48h St

Figure 8.

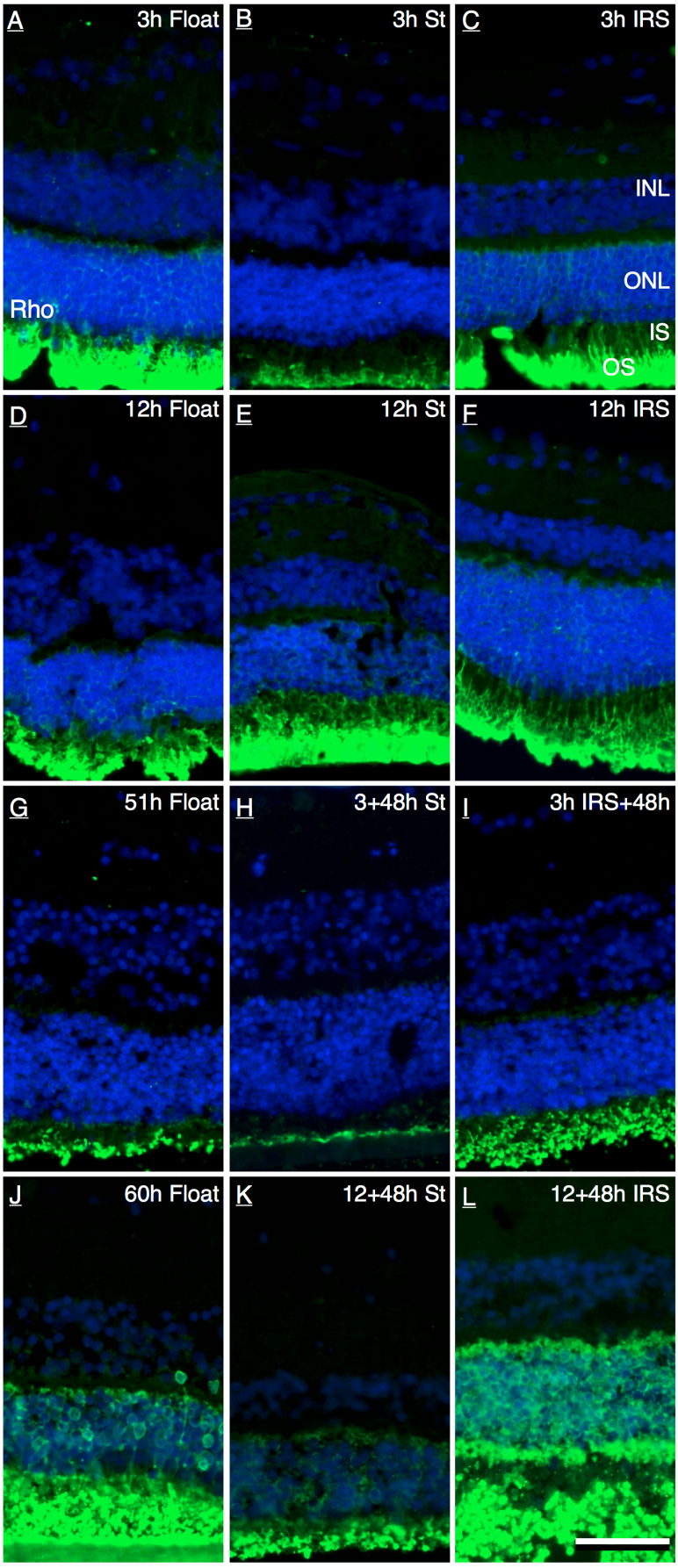
A
3h Float
B
3h St
C
3h IRS
INL
ONL
IS
OS
Rho
D
12h Float
E
12h St
F
12h IRS
G
51h Float
H
3+48h St
I
3h IRS+48h
J
60h Float
K
12+48h St
L
12+48h IRS

Figure 9.

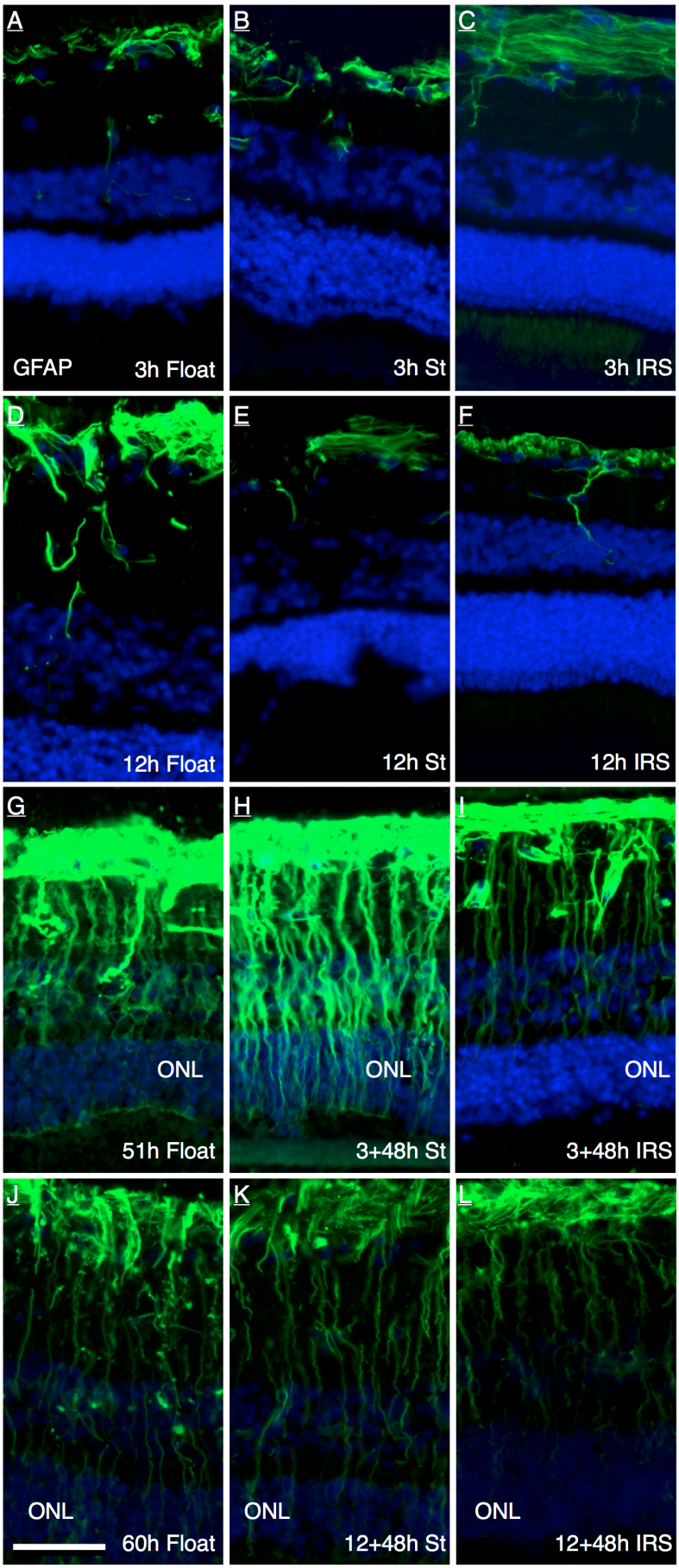
A
GFAP
3h Float
B
3h St
C
3h IRS
D
12h Float
E
12h St
F
12h IRS
G
ONL
51h Float
H
ONL
3+48h St
I
ONL
3+48h IRS
J
ONL
60h Float
K
ONL
12+48h St
L
ONL
12+48h IRS

Figure 10.

TABLES

Group name	Culture modality	Number	Culture time (h)
Baseline 1a	Free-Float	6	3
Baseline 1b	Free-Float	6	12
Baseline 2a	Standard	6	3
Baseline 2b	Standard	6	12
Baseline 3a	IRS	6	3
Baseline 3b	IRS	6	12
Detach 1a	Free-Float	6	51
Detach 1b	Free-Float	6	60
Detach/Reattach 1a	Free-Float + Standard	9	51 (3+48)
Detach/Reattach 1b	Free-Float + Standard	6	60 (12+48)
Detach/Reattach 2a	Free-Float + IRS	9	51 (3+48)
Detach/Reattach 2b	Free-Float + IRS	6	60 (12+48)

Table 1. Overview of all experimental groups. Standard cultures were maintained with photoreceptors facing the culture membrane whereas IRS (Inner Retinal Support) counterparts were kept with the innermost retina against the membrane.

Antigen	Antibody name	Target cell	Species	Dilution	Source
NeuN (Neuronal Nuclei)	Anti-neuronal nuclei	Ganglion cells	Mouse monoclonal	1:100	Millipore, USA
Cone-transducin	Anti-G protein Gγc subunit	Cone photoreceptor	Rabbit polyclonal	1:1000	Cytosignal, Ca, USA
Rhodopsin	Rho4D2	Rod photoreceptor	Mouse monoclonal	1:100	Kind gift of Prof. RS Molday, Vancouver, Canada
GFAP (glial fibrillary acidic protein	Anti-Glial Fibrillary Acidic Protein	Activated Müller cells, astrocytes	Mouse monoclonal	1:200	Chemicon International, Ca, USA
2ndary antibody	**Antibody name**	**Target**	**Species**	**Dilution**	**Source**

Antigen	Antibody name	Target cell	Species	Dilution	Source
FITC (fluorescein isothiocyanate)	Anti-mouse IgG FITC conjugate	Anti-mouse	Goat	1:200	Sigma Aldrich, St Louis, MO, USA
Texas red	Texas Red dye-conjugated AffiniPure	Anti-rabbit	Donkey	1:200	Jackson ImmunoResearch, PA, USA

Table 2. Table of primary and secondary antibodies used for immunohistochemical analysis